

Steady-State and Transient Behavior of Organic Electrochemical Transistors**

By Daniel A. Bernards and George G. Malliaras*

In recent years, organic electrochemical transistors (OECTs) have emerged as attractive devices for a variety of applications, particularly in the area of sensing. While the electrical characteristics of OECTs are analogous to those of conventional organic field effect transistors, appropriate models for OECTs have not yet been developed. In particular, little is known about the transient characteristics of OECTs, which are determined by a complex interplay between ionic and electronic motion. In this paper a simple model is presented that reproduces the steady-state and transient response of OECTs by considering these devices in terms of an ionic and an electronic circuit. A simple analytical expression is derived that can be used to fit steady-state OECT characteristics. For the transient regime, comparison with experimental data allowed an estimation of the hole mobility in poly(3,4-ethylenedioxythiophene) doped with poly(styrene sulfonate). This work paves the way for rational optimization of OECTs.

1. Introduction

The field of organic electronics has grown significantly in the past 20 years largely due to the many desirable properties of organic semiconductors such as low cost, ease of processing and tunability through synthetic chemistry.^[1] Among organic semiconductor devices, organic thin film transistors (OTFTs) have attracted considerable interest for their application in printed electronics.^[2] Within the subset of OTFTs, organic electrochemical transistors (OECTs) have distinguished themselves in recent years given their simple fabrication and low voltage operation.^[3] The ability to operate in aqueous environments and the integration with microfluidics make OECTs excellent candidates for a variety of applications, especially in the area of sensing.^[4]

OECTs were first demonstrated by White et al., where the conductivity of a poly(pyrrole) film was modulated by the application of a gate voltage through an electrolyte.^[5] Many groups have followed and demonstrated other materials and applications of OECTs.^[4] In these devices, a gate voltage is applied through an electrolyte and the conductivity of an organic semiconductor film is modulated due to the motion of ions between the electrolyte and the organic film. Being “soft” materi-

als, organic semiconductors allow significant ionic motion within their films and are particularly suited for the effects exploited in OECTs.

In general, OECTs can operate in accumulation or depletion mode; however, since the bulk of the published work deals with depletion mode operation, this is the mode considered in this paper. A prototypical semiconductor used in OECTs is poly(3,4-ethylenedioxythiophene) doped with poly(styrenesulfonate) (PEDOT:PSS), a material that is commercially available and stable under a variety of conditions. PEDOT:PSS is a degenerately doped p-type semiconductor (commonly referred to as a conducting polymer), where holes on the PEDOT are compensated by acceptors (SO_3^-) on the PSS. PEDOT:PSS OECTs have been used as logic elements,^[3i] incorporated into microfluidics,^[3k] coupled to bilayer membranes with ion channels,^[3m] as well as used for sensing of water vapor,^[3e] deoxyribonucleic acid,^[3f] and glucose.^[3g] Devices that replace the liquid electrolyte with a solid or gel electrolyte have also been fabricated and show similar behavior to solution based devices.^[3a,b,d,e,i,l] Given the wide range of applications of OECTs, it is important to understand their device physics.

Despite interest in OECTs, a comprehensive description of their current–voltage characteristics has not yet been developed. This is probably because a proper description of OECTs requires elements of electrochemistry and solid-state physics. Two models have been used to discuss the behavior of depletion mode OECTs at steady-state. The first, presented by Prigodin et al.,^[3i] approached the problem from a theoretical solid-state physics perspective. The mechanism of switching was attributed to a decrease in the hole mobility in the organic semiconductor, induced by cations that drift from the electrolyte into the organic film upon the application of a positive gate voltage. Spatially non-uniform de-doping was not considered, and no attempt was made to reproduce current–voltage characteristics. A second model, proposed by Robinson et al.,^[3n] used

[*] Prof. G. G. Malliaras, D. A. Bernards
Department of Materials Science and Engineering
Cornell University, Ithaca, New York 14853-1501
E-mail: ggm1@cornell.edu

[**] The authors acknowledge useful comments and discussions with John DeFranco, Matthew Lloyd, Jeff Mabeck, and Jason Slinker. This work was supported by the Center for Nanoscale Systems (CNS) and the Cornell Nanofabrication Facility (CNF). D. A. B. is supported by a National Defense Science and Engineering Graduate Fellowship.

arguments based on electrochemistry and electrostatics to qualitatively capture the details of OECT operation. The mechanism of switching was attributed to a decrease in the hole density in the organic film due to de-doping. An empirical relationship was assumed for the conductivity of the organic film and an assumed dopant density was used as a boundary condition. These assumptions allowed for numerical solutions of the steady-state current–voltage characteristics, which were in qualitative agreement with the experiment. These models, although very useful in highlighting important aspects of OECT physics, are not meant to allow a straightforward extraction of materials parameters from experimental data. Also, they do not treat the transient characteristics of OECTs.

In this paper we present a model that describes the behavior of depletion mode OECTs. Our model divides an OECT into an electronic circuit that accounts for hole transport in the organic semiconductor, and an ionic circuit that accounts for ion transport in the electrolyte. Using an ionic circuit equivalent to ideal polarizable electrodes, this model reproduces the steady-state and transient characteristics of PEDOT:PSS OECTs and allows the extraction of materials parameters from experimental data. The model can be easily extended to describe a variety of OECT configurations.

2. Results and Discussion

2.1. Device Model

A schematic of an OECT is shown in Figure 1. The essential components are an organic semiconductor film with source and drain contacts, an electrolyte, and a gate electrode. Because the majority of organics used for OECTs are hole transporters, the nomenclature of this analysis refers to p-type doping (mobile holes and spatially fixed acceptor ions), but it is trivial to repeat the analysis for electron transporting materials. As a convention, the source contact is grounded and a voltage is applied to the drain contact (V_d) relative to ground. The current that passes through the organic semiconductor (I_{sd}) can be monitored as a function of the applied gate voltage (V_g). Upon the application of a positive gate voltage (V_g) relative to ground, cations from the electrolyte are injected into the organic semiconductor film. This in turn de-dopes the organic semiconductor and thus decreases the source-drain current (I_{sd}).

To model device behavior the OECT is divided into an electronic and an ionic circuit. The electronic circuit consists of a p-type organic semiconductor film that transports holes between source and drain electrodes and is described by Ohm's law. Therefore, electronic transport is determined by the hole density and mobility. The ionic circuit accounts for transport of ionic charge in the electrolyte and is described as a combination of linear circuit elements. The interaction of these two components, namely the transport of ions from the electrolyte into the organic semiconductor film, is fundamental to the behavior of OECTs.

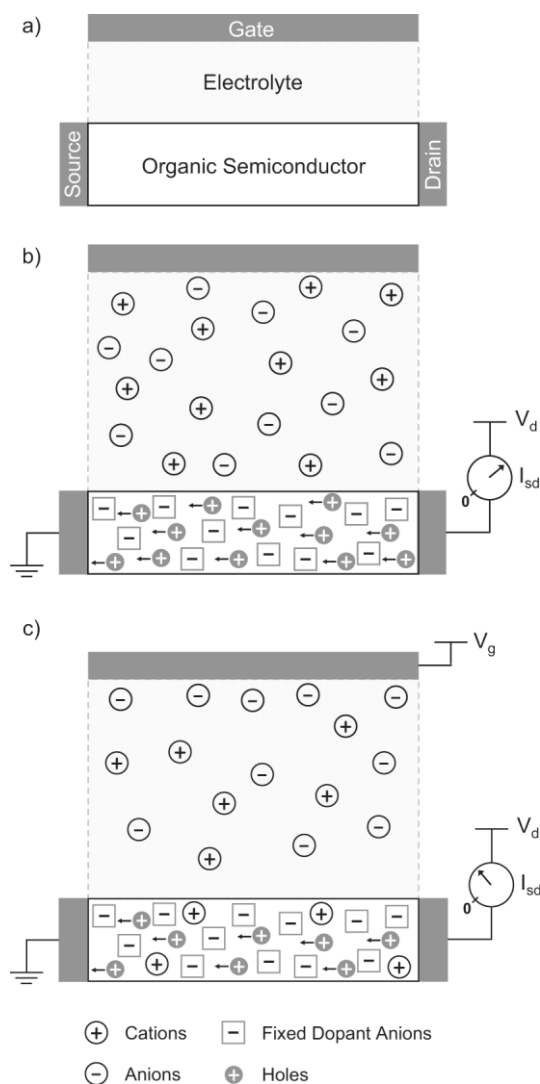


Figure 1. Qualitative representation of OECT behavior. a) OECT labeled with appropriate naming conventions. b) OECT without gate voltage applied. Current is determined by the intrinsic conductance of the organic semiconductor. c) OECT with gate voltage (V_g) applied. Current is determined by the extent to which the organic semiconductor is de-doped.

2.1.1. Electronic Circuit

The electronic circuit of an OECT is modeled using Ohm's law:

$$J(x) = q\mu p(x) \frac{dV(x)}{dx} \quad (1)$$

where J is the current flux, q is elementary charge, μ is the hole mobility, p is the hole density and dV/dx is the electric field. For this analysis, the mobility is treated as constant. This ignores the field and concentration dependence observed for organic semiconductors^[6] but simplifies the analysis significantly. Field- and/or carrier concentration-dependant mobilities can be added to the model in a straightforward way to

more accurately predict device characteristics; however, deriving analytical solutions may not be possible, requiring numerical simulations.

Upon the application of a positive gate voltage, a de-doping mechanism is used to describe carrier concentrations within the semiconductor: cations from the electrolyte are injected into the semiconductor film, and each injected cation compensates one acceptor. This is analogous to compensation doping of silicon, only it can be carried out at room temperature and at rather short time scales. De-doping in this configuration takes place as a two step process that maintains electrical neutrality in the organic semiconductor film at steady-state. For each cation that enters the organic film, a hole extracted at the source is not replaced by injection at the drain (assuming $V_d > 0$). For ease, the conductivity of the undoped organic semiconductor is assumed to be negligible. Using this framework, an expression for the effective dopant density in a volume, v , of semiconductor material will be:

$$p = p_o \left(1 - \frac{Q}{qp_o v} \right) \quad (2)$$

where p_o is the initial hole density in the organic semiconductor before the application of a gate voltage and Q is the total charge of the cations injected in the organic film from the electrolyte. For ease, the introduction of negative ions is assumed to have no effect on the organic semiconductor. To simplify the calculations, all charge densities are assumed to be uniform across the thickness of the organic semiconductor film, an approximation that limits the validity of this model to thin films.

2.1.2. Ionic Circuit

Considering the formalism of ideal polarizable electrodes from electrochemistry, the ionic circuit is described by a resistor (R_s) and a capacitor (C_d) in series.^[7] The resistor describes the conductivity of the electrolyte and is a measure of its ionic strength. The capacitor accounts for polarization at the organic film-electrolyte and gate electrode-electrolyte interfaces. Because the capacitance of the PEDOT:PSS is akin to that of a supercapacitor,^[8] it will generally be significantly greater than that of the gate (per unit area). As a result, it is expected that the properties of the gate (size, materials, etc.) will determine many device properties, including the extent of gating and the transient response time. This electrolyte model assumes that no reactions occur at the gate electrode and may not be accurate for devices where oxidation or reduction at the gate electrode is significant.^[3a,d,e,j] Equivalently, this assumes devices operate in the non-Faradaic regime, and the model might not accurately describe devices where significant Faradaic processes occur: this includes devices operating at voltages that can result in electrolysis of aqueous electrolytes.^[3g,9]

The transient behavior of this element upon the application of a gate voltage exhibits the characteristics of a charging capacitor:

$$Q(t) = Q_{ss} [1 - \exp(-t/\tau_i)] \quad (3)$$

where $Q_{ss} = C_d \Delta V$ is the total charge that passes through the circuit, ΔV is the voltage applied across the electrolyte, and the

ionic transit time is described by $\tau_i = C_d R_s$. Because C_d depends on the device area considered, it is convenient to refer to $C_d = c_d A$ for much of the analysis, where c_d is capacitance per unit area and A is the area of the device under consideration. For simplicity, the concentration and potential dependence of the ionic double layer capacitance are neglected and a constant value is assumed for c_d .

2.2. Steady-State Behavior

To solve for OECT device behavior, the effective dopant density (Eq. 2) must be spatially known throughout the organic film. If a differential slice, dx , in the vicinity of position x is considered (Fig. 2), then the charge in that slice at steady-state is related to Q_{ss} from Equation 3:

$$Q(x) = c_d \cdot W \cdot dx (V_g - V(x)) \quad (4)$$

where V_g is the gate voltage, $V(x)$ is the spatial voltage profile within the organic film and W is the width of the organic film. Using this phenomenology, de-doping can occur anywhere within the organic film and is not restricted to regions near the contacts. This is possible due to the high density of electronic charge within the organic film that can act as a source or sink for the electronic charge that results from electrochemical de-doping. Combining Equations 1–4 it is possible to obtain the governing equation for OECT characteristics at steady-state:

$$J(x) = q\mu p_o \left[1 - \frac{V_g - V(x)}{V_p} \right] \frac{dV(x)}{dx} \quad (5)$$

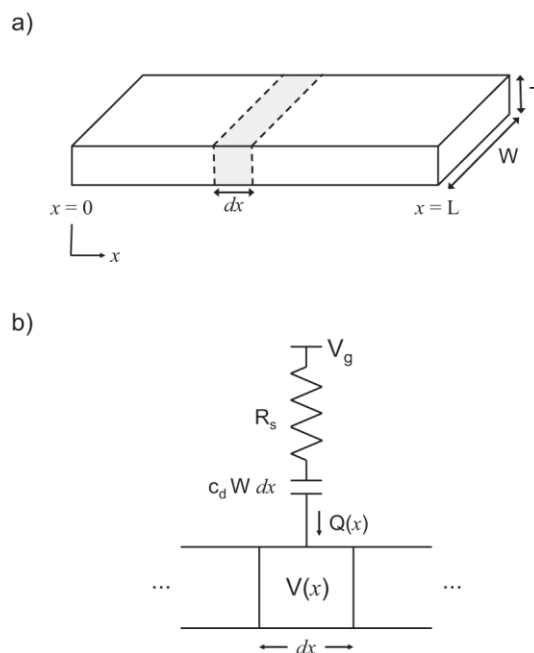


Figure 2. Device geometry used in the model. a) Organic semiconductor film with the source is located at $x=0$ and the drain at $x=L$. b) Charge (Q) from the ionic circuit is coupled to the voltage in the electronic circuit at a position x along the organic semiconductor.

where V_p is the pinch-off voltage, defined as qp_0T/c_d . At steady-state, continuity requires the source-drain current density to be spatially constant, so Equation 5 can be solved explicitly for various regimes of operation (keeping in mind that $V_g > 0$).

In the first quadrant ($V_d > 0$) there are two regimes of behavior (see Fig. 3). First, when $V_d < V_g$, de-doping will occur everywhere in the organic film. Using the previous assumptions, Equation 5 can be rewritten in terms of current and then solved explicitly, placing the source at $x=0$ and the drain at $x=L$:

$$I = G \left[1 - \frac{V_g - 1/2V_d}{V_p} \right] V_d \quad (6)$$

where G is the conductance of the organic semiconductor film ($G = q\mu p_0 WT/L$).

The second regime occurs when $V_d > V_g$, and de-doping will only occur in the region of the device where $V(x) < V_g$. This regime is described by:

$$I = G \left[V_d - \frac{V_g^2}{2V_p} \right] \quad (7)$$

where the current is linear with drain voltage, and the onset of linear behavior occurs when $V_d = V_g$.

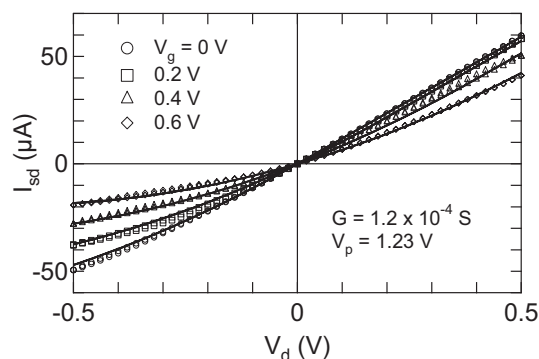


Figure 3. Experimental steady-state current–voltage characteristics (data points) for an OEET fitted to modeled steady-state current–voltage characteristics (solid lines) with $G = 1.2 \times 10^{-4}$ S and $V_p = 1.23$ V. 10 mM NaCl solution was used as the electrolyte and the organic film dimensions were $L = 5$ mm and $W = 6$ mm.

In the third quadrant ($V_d < 0$), it is possible to completely de-dope portions of the organic film when the local density of injected cations becomes equal to the intrinsic dopant density of the semiconductor material. Mathematically this is true when $(V_g - V_d) \geq V_p$, where the critical drain voltage for saturation can be written as $V_d^{\text{sat}} = V_g - V_p$. Locally the semiconductor will be depleted near the drain contact, but holes injected into this region will still be transported to the drain. An equivalent argument is used to describe saturation in depletion-mode field effect transistors.^[10]

If the magnitude of V_d increases beyond V_d^{sat} , the extent of the depleted region will move slightly toward the source. For organic films that are sufficiently long, the location of the

depleted region nearest the source contact will not change appreciably with V_d and the source-drain current will saturate. If the extent of the depletion region moves significantly with variation in V_d , the current will not saturate but continue to increase—an effect that can be observed in devices with short source-drain spacing.^[3h] In the limit of long channels, for $V_d \leq V_d^{\text{sat}}$, the current will only depend on the drain voltage at saturation for a particular gate voltage:

$$I = \frac{G \cdot V_d^{\text{sat}^2}}{2V_p} \quad (8)$$

Complete de-doping at $V_d > 0$ is also possible and first occurs when $V_g = V_p$. The behavior in this regime can be determined using equivalent device representations but is typically not of significant interest because of the high gate voltages required. For devices operating at saturation, spatial voltage profiles can not be analytically be determined in this regime of device operation.

Experimental steady-state current–voltage characteristics for a PEDOT:PSS OEET are shown in Figure 3 (device details are described in the experimental section). An excellent fit to this data is obtained using the model (solid lines). Such a fit relies on two parameters. The first one is the conductance of the organic semiconductor film ($G = q\mu p_0 WT/L$), which can easily be determined independently with conventional techniques. The second parameter is the pinch-off voltage ($V_p = qp_0T/c_d$) and is a measure of the dopant density of the semiconductor film relative to the ionic charge that is leveraged from solution for de-doping. The pinch-off voltage indicates the onset of saturation in the absence of a gate bias and is akin to the pinch off voltage in conventional depletion mode field effect transistors.^[11]

To further assess the model, it was applied to reproduce the steady-state characteristics of PEDOT:PSS OEETs reported in literature.^[3h,j,k,n] Fitting to experimental data (including the results presented here) yielded PEDOT:PSS conductivities in the range of 20–100 S cm^{-1} and pinch-off voltages in the range of 0.5–2 V (for devices with aqueous electrolytes). Using typical values for double layer capacitance (10–40 $\mu\text{F cm}^{-2}$),^[7] hole densities of 10^{19} – 10^{20} cm^{-3} were extracted, which is consistent with what is expected in highly doped organic semiconductors.^[12] Since this value is obtained using electrostatic arguments, it should be interpreted as the total density of holes in the HOMO manifold of PEDOT. One should keep in mind that only a small fraction of these holes (the ones that are close to the Fermi level) will be mobile at experimental time scales.^[6c] In general, the model adequately describes spatial voltage profiles but cannot be used for devices operated at saturation due to the limitations of the derivation. Consequently, it is difficult to compare the model results to some of the experimentally measured voltage profiles.^[3n]

The characteristic steady-state behavior reproduced here assumes that steady-state has been reached after the application of a gate voltage. This is not necessarily the case if conventional voltage sweep measurements are used, and this may account for some deviations from the model at high gate voltages.^[3c,h,j,k,n] Another non-ideality arises in many realistic

applications where the organic semiconductor used for an OECT is sufficiently conductive that it can be used as leads, interconnects, or contacts to the organic film.^[3a-e,j,l,n] In some configurations, a significant voltage may drop across regions of material that are not gated. This is equivalent to the addition of a series resistance in the electronic circuit, and it is straightforward to account for such realistic device configurations with the presented model. For example, the addition of a series resistance that is symmetric about the active region yields device characteristics that can be explicitly calculated by appropriately modifying Equation 5. This effect is presented in Figure 4. Deviations from ideal behavior include a larger negative voltage required for the onset of saturation and reduced gating

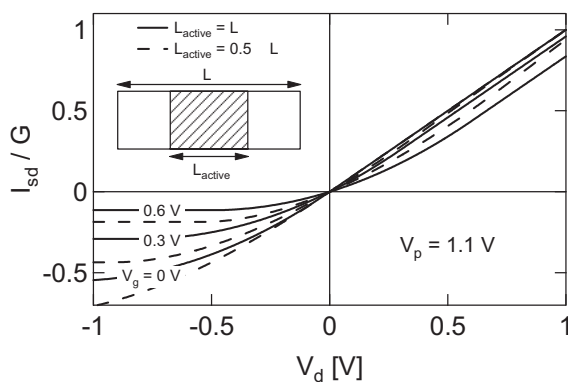


Figure 4. Comparison of simulated steady-state current–voltage characteristics for an ideal device geometry (solid lines) and for a device with an additional series resistance (dashed lines) with $V_p = 1.1$ V.

under positive drain voltage. Furthermore, it is possible to suppress gating at large positive drain voltages if the applied gate voltage is less than the voltage within the active (gated) region.

In addition to transistors or logic elements, OECTs have been used for many sensing applications.^[4] For these devices it is important to understand the relative, rather than absolute, device response upon gating. Namely, the relevant parameter is $\Delta I_{sd}/I_{sd}$ where ΔI_{sd} is the change in current upon application of a gate voltage. As shown in Figure 5, the relative device re-

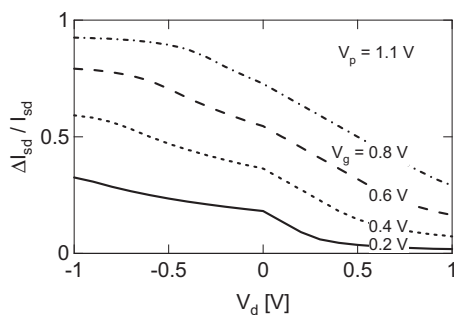


Figure 5. Normalized simulated steady-state current as a function of drain voltage for a series of gate voltages with $V_p = 1.1$ V, where I_{sd} is the source-drain current without an applied gate voltage and ΔI_{sd} is the change in source-drain current upon the application of a gate voltage.

sponse increases with increasing gate voltage, especially at negative drain voltages. Such characteristics are paramount in developing high sensitivity sensors and are a useful tool in determining optimal device operating conditions.

2.3. Transient Behavior

The transient behavior of OECTs will be dominated by two effects: injection of a cation from the electrolyte into the organic film and removal of a hole at the source electrode ($V_d > 0$). In order to make a calculation of the transient response tractable, the spatial variation of the voltage and the hole density are ignored and an average ionic current and hole density are used. By accounting for the current associated with the removal of holes due to de-doping in addition to that from Ohm's law, the simplified behavior can be described by:

$$J(t) \approx q\mu p(t) \frac{V_d}{L} + qfL \frac{dp(t)}{dt} \quad (9)$$

where f is a proportionality constant to account for the spatial non-uniformity of the de-doping process. The characteristic range for f is 0 (for instance when $V_d \gg V_g$ at positive V_d) to 1/2 (for instance when $V_g \gg V_d$). Much of the complexity of the time dependant response is incorporate into f , which is expected to depend on the gate and drain voltages.

Using Equation 2, the transient response in Equation 9 can be determined exactly:

$$I(t) \approx G \left(1 - \frac{Q(t)}{qp_0 v} \right) V_d - f \frac{dQ(t)}{dt} \quad (10)$$

where $Q(t)$ is the transient response of the relevant ionic circuit. Two experimental conditions can be considered when solving for the response of the ionic circuit: constant gate current and constant gate voltage. While constant gate current is not a typical operating regime, it is a useful one for understanding device physics. By forcing a constant current through the electrolyte, the kinetics of the ionic circuit can be fixed. In essence, constant gate current experiments shift the focus to the electronic behavior of the OECT. Plugging in the appropriate parameters for constant gate current (I_g), the transient behavior simplifies to:

$$I(t, I_g) = I_o - I_g \left(f + \frac{t}{\tau_c} \right) \quad (11)$$

where I_o is the source-drain current prior to application of a gate current and the electronic transit time is described by $\tau_c = L^2/\mu V_d$. This equation is a useful tool to verify the transient model irrespective of the ionic circuit that is chosen. Additionally, this provides a simple route to extract an effective hole mobility in the organic semiconductor film.

Typical constant gate current transient response characteristics are shown in Figure 6, which agree with the predicted dependence in Equation 11. This supports the assumptions used for the transient model. Plotting the slope of the source-drain transient in Figure 6 as a function of gate current (Fig. 6, inset), it is possible to extract τ_c for this device. The data of Figure 6 reveal a hole mobility for PEDOT:PSS in the range of 10^{-2} –

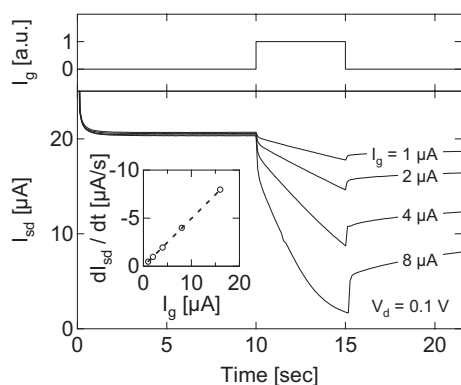


Figure 6. Experimental transient response of an OEET under application of a constant gate current. (Inset) The transient slope of source-drain current is plotted versus gate current, which predicts $\tau_e = 0.5$ s. 1 M NaCl solution was used as the electrolyte and the organic film dimensions were $L = 0.5$ mm and $W = 6$ mm.

10^{-3} cm² V⁻¹ s⁻¹. These values are on the high side for conjugated polymers, which is expected due to the high level of doping.^[6b] Since this experiment measures the “time-of-flight” of holes, the mobility should be interpreted as that of holes near the Fermi level.^[6c] It should be noted that upon removal of the applied gate current, there is a slow recovery of the source-drain current. This is most likely due to diffusion of cations from the semiconductor film back into the electrolyte.

In order to consider the transient behavior under constant gate voltage, the electrolyte model described above (Eq. 3) is applied. For simplicity, the transient behavior is only described for the case where de-doping occurs everywhere within the organic film without saturation effects. An average voltage drop between the organic film and the gate electrode ($\Delta V = V_g - 1/2 V_d$) is chosen to ensure that transient behavior is consistent with steady-state characteristics. Using these assumptions, the transient behavior for a simplified OEET can be described as:

$$I(t, V_g) = I_{ss}(V_g) + \Delta I_{ss} \left(1 - f \frac{\tau_e}{\tau_i}\right) \exp(-t/\tau_i) \quad (12)$$

where $I_{ss}(V_g)$ is the steady-state source-drain current at a gate voltage V_g and $\Delta I_{ss} = I_{ss}(V_g = 0) - I_{ss}(V_g)$. This gives rise to a unique transient behavior as shown in Figure 7. Namely, the

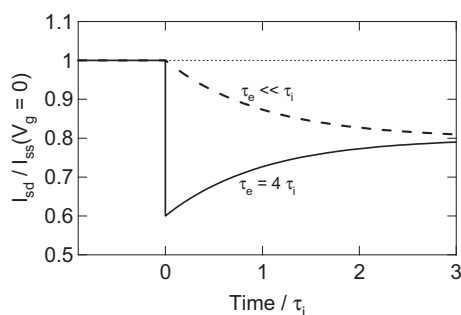


Figure 7. Modeled source-drain current transient for a constant drain voltage with an arbitrary ΔI and fixed geometric factor ($f = 1/2$). Transient demonstrates two different possible characteristics responses.

approach to steady-state for an OEET in response to an applied gate voltage can be either a monotonic decay ($\tau_i > f\tau_e$) or a spike-and-recovery ($\tau_i < f\tau_e$). Qualitatively, a monotonic decay indicates the electronic response of the organic film (i.e., how quickly holes can be extracted from the film) is sufficiently fast that it can be ignored when considering the overall transient response. This is typically the case for devices with small source-drain spacing and/or large drain voltages. A spike-and-recovery indicates that hole transport in the organic film occurs at a relatively slow rate and the transient current is dominated by hole extraction from the film.

From Equation 12, it is apparent that the transient response of an OEET can be characterized primarily by two parameters (τ_i and τ_e) that describe underlying time scales for transport. The characteristic time constant for ionic transport in the electrolyte (τ_i) is determined by the solution resistance and capacitance of the ionic double layer. Using Gouy–Chapman theory for double layer capacitance (neglecting voltage dependence) along with linear solution conductivity, $\tau_i \sim lC^{1/2}$, where l is distance between the organic film and gate electrode and C is the ionic concentration.^[7] Qualitatively, decreasing the gate electrode distance from the channel or increasing electrolyte concentrations will lead to improved device response times, which agrees qualitatively with our experimental observations. The characteristic electronic time constant (τ_e) described previously is also relevant for describing the transient response. Since the character of Equation 12 is determined chiefly by the ratio τ_e/τ_i , it is important to note that $\tau_e/\tau_i \sim lL^2/\mu V_d$. From this relationship, it is apparent that the character of the transient response can be modulated in a straightforward way by varying the electrode location, the organic film length or the drain voltage. For example, by varying the applied source-drain voltage, the character of the transient can be altered as shown in Figure 8. As expected, the transient changes from a monotonic decay to a spike-and-recovery with decreasing V_d .

Finally, the model can be easily modified to describe OEETs as transducers in sensing applications. For instance, lipid mem-

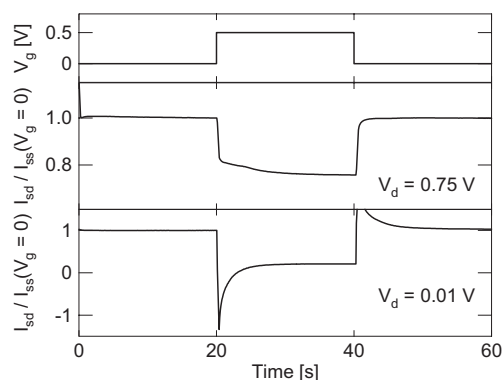


Figure 8. Experimental source-drain current transient with constant applied gate voltage. Source-drain current is normalized to the source-drain current prior to applied gate voltage [$I_{sd}(V_g = 0)$]. Two characteristic responses can be observed with variation in V_d . 10 mM NaCl solution was used as the electrolyte and the organic film dimensions were $L = 5$ mm and $W = 6$ mm.

branes with ion channels have been characterized by specific equivalent ionic circuits in literature.^[13] Using such circuits in conjunction with the proposed model can be used as a tool to improve the devices or sensors that integrate ion channels and OECTs.^[3m]

3. Conclusions

In this paper we have presented a model that describes the steady-state and transient behavior of OECTs. Utilizing a two circuit approach, the ionic and electronic nature of OECTs was accounted for and realistic device behavior was reproduced. The model showed excellent agreement when used to fit typical device behavior at steady-state. The source-drain current transient was predicted to exhibit two types of characteristic behavior: monotonic decay or spike-and-recovery. Both types of response were demonstrated in a PEDOT:PSS OECT by variation of the drain voltage. The model shows how tuning of the appropriate device parameters can be used as a means to minimize the response time of OECTs. Typical materials parameters extracted from comparison with experiment were reasonable estimates for the mobility of PEDOT:PSS. In general, this simple model is a powerful tool for design of OECTs, which can be modified to account for many variations in device design.

4. Experimental

The organic layer used for all OECTs was the commercial polymer Baytron P, poly(3,4-ethylenedioxythiophene) doped with poly(styrene-sulfonate) (PEDOT:PSS). A mixture of Baytron P and ethylene glycol (4:1 by volume) was spun coated onto clean glass slides to yield films approximately 50 nm thick. Substrates were cleaned mechanically with deionized water and detergent and primed with acetone and isopropanol to improve film formation. To reduce background resistance, either gold was evaporated or silver paint was applied to inactive regions of the organic film. Commercial Sylgard 184, poly(dimethylsiloxane), was mixed at a 10:1 base to cross-linker ratio and cured at 60 °C for 1 h prior to being used to define electrolyte wells. NaCl was mixed with deionized water to obtain electrolyte solutions in the range of 10 mM to 1 M. Either a Pt or Ag/AgCl wire was used as the gate electrode. All

measurements were taken using Kiethley 2400 source-measure units controlled by Labview software customized for each experiment.

Received: December 22, 2006

Revised: March 13, 2007

Published online: October 16, 2007

- [1] G. Malliaras, R. Friend, *Phys. Today* **2005**, *58*, 53.
- [2] C. D. Dimitrakopoulos, P. R. L. Malenfant, *Adv. Mater.* **2002**, *14*, 99.
- [3] a) P. Andersson, D. Nilsson, P.-O. Svensson, M. Chen, A. Malmström, T. Remonen, T. Kugler, M. Berggren, *Adv. Mater.* **2002**, *14*, 1460. b) A. J. Epstein, F.-C. Hsu, N.-R. Chiou, V. N. Prigodin, *Curr. Appl. Phys.* **2002**, *2*, 339. c) J. Lu, J. Pinto, A. G. MacDiarmid, *J. Appl. Phys.* **2002**, *92*, 6033. d) D. Nilsson, M. X. Chen, T. Kugler, T. Remonen, M. Armgarth, M. Berggren, *Adv. Mater.* **2002**, *14*, 51. e) D. Nilsson, T. Kugler, P. O. Svensson, M. Berggren, *Sens. Actuators B* **2002**, *86*, 193. f) K. Krishnamoorthy, R. S. Gokhale, A. Q. Contractor, A. Kumar, *Chem. Commun.* **2004**, 820. g) Z. T. Zhu, J. T. Mabeck, C. C. Zhu, N. C. Cady, C. A. Batt, G. G. Malliaras, *Chem. Commun.* **2004**, 1556. h) M. M. Alam, J. Wang, Y. Guo, S. P. Lee, H.-R. Tseng, *J. Phys. Chem. B* **2005**, *109*, 12777. i) S. Ashizawa, Y. Shinohara, H. Shindo, Y. Watanabe, H. Okuzaki, *Synth. Met.* **2005**, *153*, 41. j) D. Nilsson, N. Robinson, M. Berggren, R. Forchheimer, *Adv. Mater.* **2005**, *17*, 353. k) J. T. Mabeck, J. A. DeFranco, D. A. Bernards, G. G. Malliaras, S. Hocde, C. J. Chase, *Appl. Phys. Lett.* **2005**, *87*, 013 503. l) V. N. Prigodin, F. C. Hsu, Y. M. Kim, J. H. Park, O. Wladmann, A. J. Epstein, *Synth. Met.* **2005**, *153*, 157. m) D. A. Bernards, G. G. Malliaras, G. E. S. Toombes, S. M. Gruner, *Appl. Phys. Lett.* **2006**, *89*, 053 505. n) N. D. Robinson, P. O. Svensson, D. Nilsson, M. Berggren, *J. Electrochem. Soc.* **2006**, *153*, H39.
- [4] J. T. Mabeck, G. G. Malliaras, *Anal. Bioanal. Chem.* **2006**, *384*, 343.
- [5] H. S. White, G. P. Kittleson, M. S. Wrighton, *J. Am. Chem. Soc.* **1984**, *106*, 5375.
- [6] a) P. M. Borsenberger, L. Pautmeier, H. Bassler, *J. Chem. Phys.* **1991**, *94*, 5447. b) P. W. M. Blom, M. J. M. de Jong, M. G. van Munster, *Phys. Rev. B* **1997**, *55*, R656. c) Y. Shen, K. Diest, M. H. Wong, B. R. Hsieh, D. H. Dunlap, G. G. Malliaras, *Phys. Rev. B* **2003**, *68*, 081 204.
- [7] A. J. Bard, L. R. Faulkner, *Electrochemical Methods*, Wiley, New York **1980**.
- [8] J. D. Stenger-Smith, C. K. Webber, N. Anderson, A. P. Chafin, K. Zong, J. R. Reynolds, *J. Electrochem. Soc.* **2002**, *149*, A973.
- [9] F. Lin, M. C. Lonergan, *Appl. Phys. Lett.* **2006**, *88*, 133 507.
- [10] a) W. Shockley, *Proc. IRE* **1952**, *40*, 1365. b) A. S. Grove, *Physics and Technology of Semiconductor Devices*, Wiley, New York **1967**.
- [11] a) J. T. Wallmark, *RCA Rev.* **1963**, *24*, 641. b) R. D. Middlebrook, *Proc. IEEE* **1963**, *51*, 1146.
- [12] Handbook of Conducting Polymers (Eds: T. A. Skotheim, R. L. Else-nbaumer, J. R. Reynolds), Marcel Dekker, New York **1998**.
- [13] *Planar Lipid Bilayers (BLMs) and Their Applications* (Eds: H. T. Tien, A. Ottova-Leitmannova), Elsevier, Amsterdam **2003**.